Supramolecular Catalysis

DOI: 10.1002/anie.201203768

Mechanistic Insights into a Supramolecular Self-Assembling Catalyst System: Evidence for Hydrogen Bonding during Rhodium-Catalyzed Hydroformylation**

*Urs Gellrich, Wolfgang Seiche, Manfred Keller, and Bernhard Breit**

The hydroformylation of olefins is one of the most important applications of homogeneous catalysis in industry, annually producing millions of tons of aldehydes.[1] The selectivity towards the desired linear aldehyde is usually achieved by crafting the microenvironment of the catalytically active metal species through the binding of appropriate ligand architectures. Amongst the many ligands developed for this process, bidentate phosphines with a wide bite angle such as Xantphos (**2**; Scheme 1) are particularly effective because of

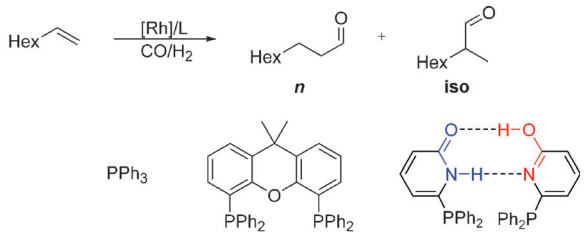

L	1	2	3 dimer
n: iso	75:25	98:2	96:4
TOF [h^{-1}]	1270	730	3350

Scheme 1. Selectivity and activity observed in the rhodium-catalyzed hydroformylation of 1-octene with various ligands. Conditions: Rh/L/substrate = 1:20(10):7500, 80 °C, 10 bar, toluene.

their high regioselectivity for the linear aldehyde (high *n*/iso ratio).[2] Previously, we demonstrated that monodentate phosphorus ligands possessing hydrogen-bond recognition motifs are able to achieve levels of selectivity previously only attained with bidentate ligands, together with outstanding activities.[3,4] The most prominent example of such supramolecular self-assembling ligands is the 6-diphenylphosphinopyridin-2-(1*H*)-one (6-DPPon; **3**) system. Its exceptional activity and selectivity in the hydroformylation of terminal alkenes allows reactions to be carried out at room temperature and ambient pressure.

This has enabled the development of tandem processes such as a tandem hydroformylation/asymmetric organocatalytic cross-aldol reaction.[5] More recently, the utility of this system was demonstrated by the devlopement of a highly selective tandem hydroformylation/hydrogenation process.[6] The hydrogen-bonding properties of this ligand system have been intensively studied in a $[Cl_2Pt(\mathbf{3})_2]$ complex.[7] However, evidence that the proposed hydrogen-bonding interaction occurs during the catalytic reaction was lacking. Herein, we present a mechanistic investigation that proves the existence of hydrogen bonding during the catalytic cycle, and demonstrate its importance for catalyst activity and selectivity. We were able to characterize an intermediate of the catalytic cycle, the acyl complex $[(COR)Rh(\mathbf{3})_2(CO)_2]$, and demonstrate its catalytic competence.

Our investigation commenced with attempts to prepare an analogue to the Wilkinson complex. Pleasingly, the reaction of $[Rh(CO)_2(acac)]$ (acac = acetylacetanoate) with ligand **3** under syngas pressure furnished $[HRh(\mathbf{3})_3CO]$ (**4**) in 80% yield as an orange crystalline compound. Thorough ^1H, ^{31}P, ^{103}Rh NMR and IR spectroscopic studies indicated the presence of hydrogen bonds between one ligand in the hydroxypyridine form and one ligand in the pyridone form. Furthermore, detailed analysis of variable-temperature NMR spectra showed that the rhodium complex **4** exists as a dimer, the structure of which could be determined by X-ray diffraction (Figure 1).

By pressurizing complex **4** with CO (4 bar) we were able to detect the formation of $[HRh(\mathbf{3})_2(CO)_2]$ (**5**) by in situ IR spectroscopy. DFT calculations enabled the vibrations of this complex to be assigned to equatorial/equatorial (eqeq) and axial/equatorial (axeq) conformers, and are in good agreement with those observed experimentally. A broad absorption between 2300 cm^{-1} and 3500 cm^{-1} corresponds to the O–H···O and N–H···N vibrations of the hydrogen-bonding network. The unusual shape of these vibrations is caused by a fast double-proton transfer process, which is in accordance with our previous studies on the $[Cl_2Pt(\mathbf{3})_2]$ complex.[6] Complex **5** was also produced by the reaction between $[Rh(CO)_2(acac)]$ and 10 equiv **3** in a CO/H_2 atmosphere and was identified as the resting state of the catalytic transformation through in situ IR spectroscopy.[8] This finding indicates, in agreement with kinetic studies, which show a first order dependency of the TOF on the alkene concentration, an early rate-determining step in the catalytic cycle.[9] To gain

[*] U. Gellrich, Dr. W. Seiche, Dr. M. Keller, Prof. Dr. B. Breit
Institut für Organische Chemie und Biochemie
Freiburg Institute for Advanced Studies (FRIAS)
Albert-Ludwigs-Universität Freiburg
Albertstrasse 21, 79104 Freiburg i. Brsg. (Germany)
E-mail: bernhard.breit@chemie.uni-freiburg.de

[**] Support from the Freiburg Institute for Advanced Studies (FRIAS), the Deutsche Forschungsgemeinschaft (IRTG 1038), and the Fonds der chemischen Industrie (PhD fellowship to U.G.) is gratefully acknowledged. We thank S. Diezel for support with the kinetic experiments, J. Schäfer for help with X-ray structure analysis, and Dr. M. Cooke and Prof. Dr. D. Plattner for stimulating discussions.

Supporting information for this article is available on the WWW under http://dx.doi.org/10.1002/anie.201203768.

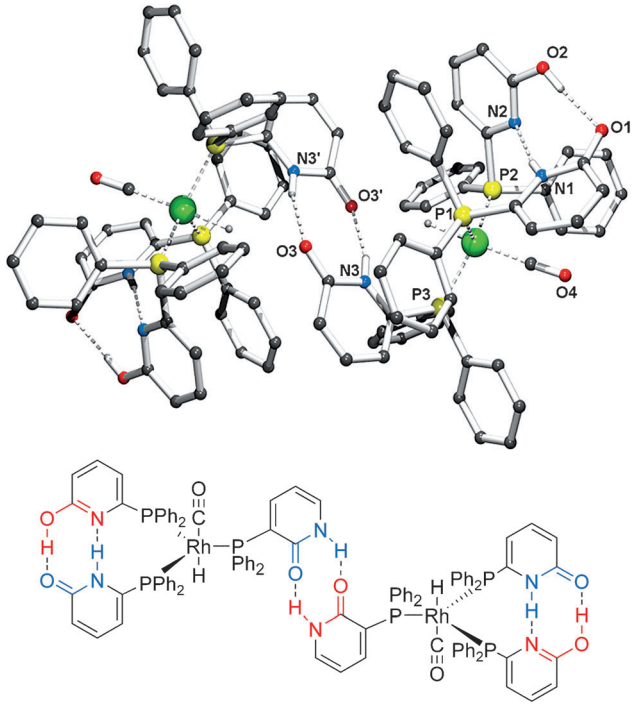

Figure 1. X-ray structure of the [HRh(6-DPPon)$_3$(CO)] (**4**) complex. Selected bond lengths [Å] and angles [°]: N–H···O: 2.880(3), 164(3); O–H···O: 2.657(3), 170(4); N–H···N: 2.892(3), 169(3); P-Rh-P: 115.23(3).

a deeper insight into the mechanism we performed a detailed DFT study on the catalytic cycle (Figure 2).[10] Several conformers (e.g. *cis*/*trans* and eqeq/axeq) and tautomers were optimized for each intermediate and transition state (TS). Propene was used as a model for the 1-octene used experimentally. Despite the fact that many previous studies have focused on the TS for hydrometalation,[11] less attention has been paid to alkene coordination.[12] We were able to locate and optimize transition states for alkene coordination, but the hydrometalation remains rate-determining on the computed ΔG surface (Figure 2).

Comparison of the DFT-optimized hydrogen-bond geometries of the pentacoordinated [HRh(**3**)$_2$(CO)$_2$] (**5**) complex (P-Rh-P: 112°) and the catalytically active species *trans*-[HRh(**3**)$_2$(CO)] (**6**; P-Rh-P: 154°) shows an elongation of the N–H···N bond by 0.5 Å in the latter (Figure 3). In contrast, the O–H···O bond length remains unchanged. This observation indicates that the N–H···N bond corresponds to the flexible part of the hydrogen-bonding network, whereas the O–H···O bond is responsible for the chelating character of the ligand backbone.[13] This synergism of flexibility and structural integrity is likely to be a key for understanding the exceptional high activity of this ligand compared to covalently bound bidentate ligands, since it facilitates the adoption of different coordination geometries and bite angles without severe energy penalties. In agreement with this assumption,

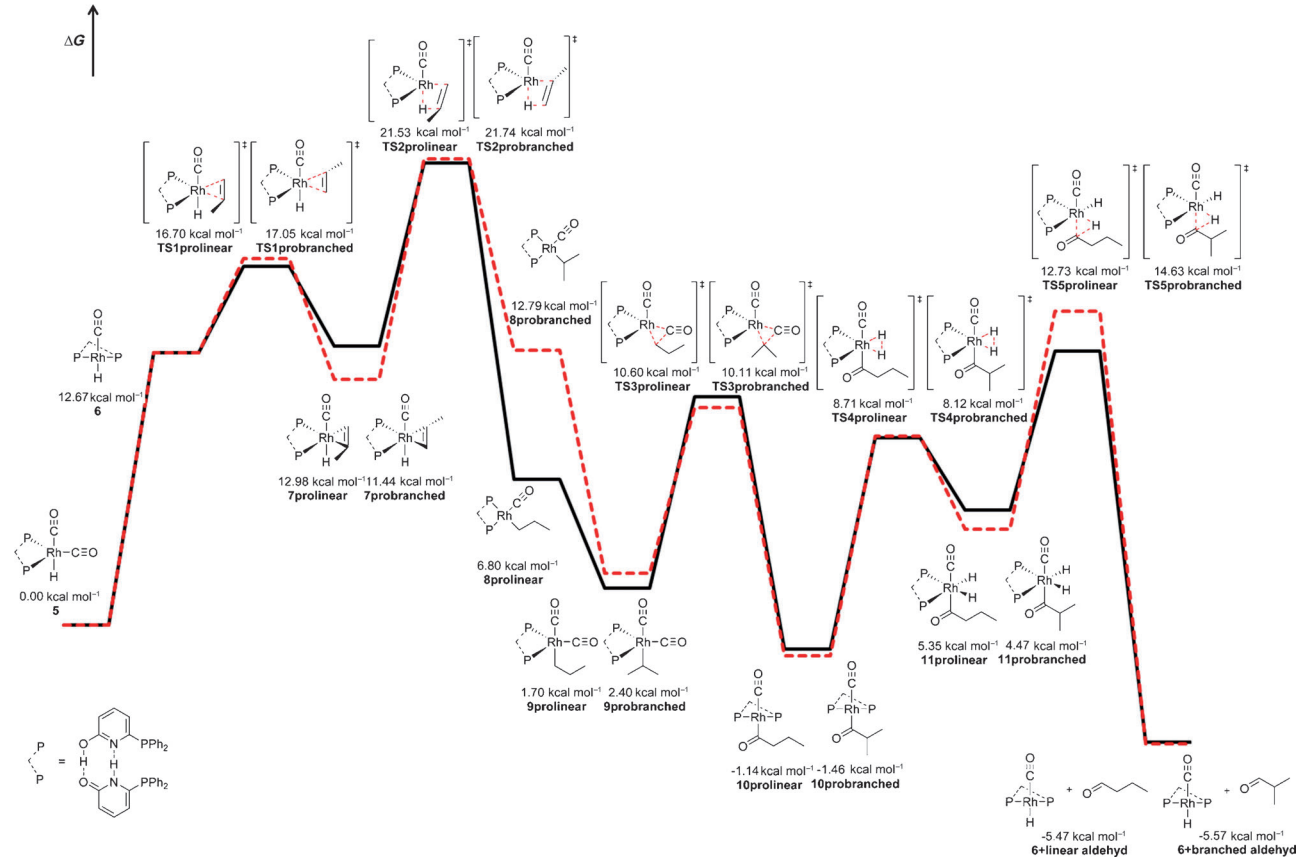

Figure 2. Free energy surface of the catalytic cycle (M06/6-311 + G(2d,p)[C,H,N,O,P] + SDD[Rh] using the PCM model for toluene on B3LYP/6-31G(d,p)[C,H,N,O,P] + LANL2DZ[Rh]-optimized structures. Thermodynamic corrections were obtained from a frequency calculation at the B3LYP level).

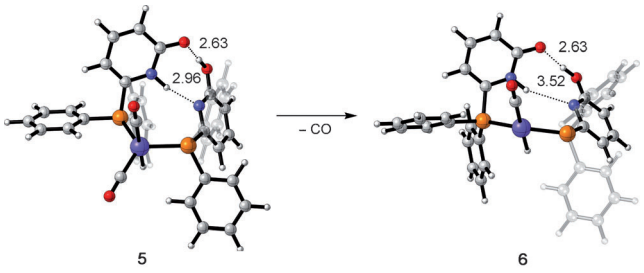

Figure 3. B3LYP-optimized structures and hydrogen-bond lengths of the resting state (**5**) and the actually catalytic active species, the *trans*-[HRh(**3**)$_2$(CO)] (**6**) complex.

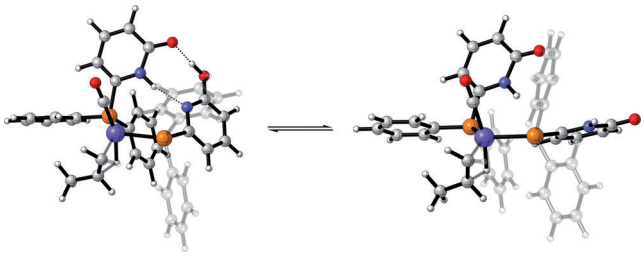

Figure 4. B3LYP-optimized structures for the TS of the prolinear hydrometalation with hydrogen bonds (left), and a conformer where hydrogen bonding is prevented for geometrical reasons (right).

the reported lowest energy pathways for the Xantphos- and Thixantphos-catalyzed hydroformylation involves *cis*-coordinated hydride species.[2,14]

Interestingly, the lowest TS for the prolinear hydrometalation and the probranched hydrometalation do not start from the same alkene complex, which was confirmed by IRC calculations (Figure 2).[15] The prolinear alkene complex is higher in energy, and therefore the resulting ΔG^{TS} value is smaller; this is an interesting example of the concept of survival of the weakest.[16] The *n*/iso ratio, calculated from the two different ΔG^{TS} values, is in good agreement with the experimental observations (Table 1).[17] The computed free energy surface shows that the prolinear hydrometalation step is exothermic ($\Delta G_r = -6.18$ kcal mol^{-1}) whereas the probranched hydrometalation is slightly endothermic ($\Delta G_r =$ 1.35 kcal mol^{-1}).

Table 1: Comparison of the computed selectivity and the experimentaly obtained selectivity.

	B3LYP[a]	M06[b]	Expt.
$\Delta\Delta G^{TS}$ [kcal mol^{-1}]	1.17	1.75	–
n/iso	88:12	95:5	96:4

[a] 6-31G(d,p)[C,H,N,O,P] + LANL2DZ[Rh]. [b] 6-311 + G(2d,p)-[C,H,N,O,P] + SDD[Rh] (PCM for toluene).

In agreement with the computed reaction enthalpies, deuteroformylation experiments reveal that deuterium incorporation occurs only in the C1-position of the alkene after 20% conversion, thus indicating that the probranched hydrometalation is reversible.[18] However, it is likely that the reversibility depends on the CO pressure since the dicarbonyl species **9** is thermodynamically favored, which is reflected in a lower regioselectivity at higher pressures.[19] Therefore, the regioselectivity seems to be due to a combination of kinetic and thermodynamic control. We then focused on the optimization of several transition states for hydrometalation in which hydrogen bonding is prevented by geometrical constraints (Figure 4). In these transition states the pyridone tautomer is favored, which agrees with previous investigations.[7] However, M06 and B3LYP calculations predict that hydrogen bonding stabilizes the rate-determining TS by at least 7 kcal mol^{-1} (Figure 4).

To get additional experimental proof for the importance of the hydrogen-bond network for the outstanding selectivity and activity, we synthesized O- and N-methylated derivatives of **3** (**12** and **13**) so as to prevent the possibility of hydrogen bonding and then evaluated them in the hydroformylation of 1-octene under identical conditions (Scheme 2).[20] Indeed **12** and **13** showed selectivities comparable to classical monodentate ligands such as PPh_3 (**1**). Furthermore, the reactions with **12** and **13** were significantly slower than with the 6-DPPon (**3**) catalyst, thus highlighting the importance of the hydrogen bonds for the outstanding activity.

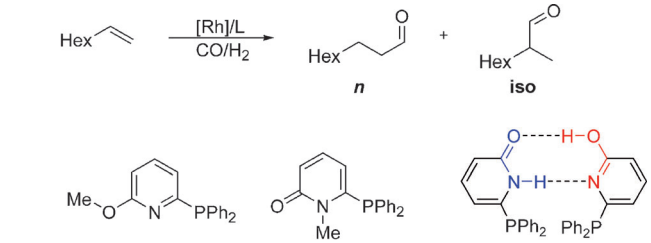

Scheme 2. Selectivity observed in the rhodium-catalyzed hydroformylation of 1-octene with various ligands. Conditions: Rh/L/substrate = 1:20:7500, 80 °C, 10 bar, toluene.

To further validate the presence of hydrogen bonds during the catalytic reaction, we performed in situ IR experiments starting from isolated **4**. After pressurizing this complex with CO (4 bar) the spectrum of complex [HRh(**3**)$_2$(CO)$_2$] (**5**) was substracted. The formation of an intermediate was observed upon addition of 1.5 equiv 1-octene under CO pressure (4 bar). This intermediate shows a strong absorption at 1663 cm^{-1}, which indicates the formation of a rhodium–acyl complex (Figure 5).[21] DFT computations were performed to assign the emerging vibrations (Table 2).

After correction for anharmonicity, the computed vibrations were found to be in good agreement with the experimental observations (Table 2). This finding suggests that the complex formed is a rhodium–acyl complex bearing two 6-DPPon (**3**) ligands. To validate that a catalytically active intermediate was formed, not a thermodynamically stable, unreactive complex, we then pressurized the solution with CO/H_2 (4 bar), which immediately resulted in the formation of nonanal, as indicated by the appearance of its CO

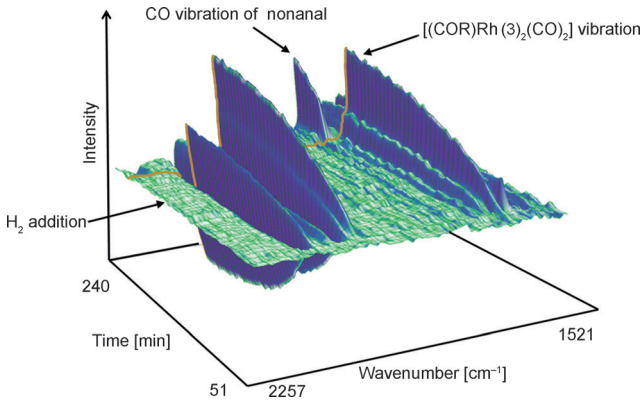

Figure 5. Difference in situ IR spectra obtained after the addition of 1.5 equiv 1-octene under CO pressure to the solution of the $[HRh(\mathbf{3})_2(CO)_2]$ complex (10^{-2} M in toluene). The orange line marks the addition of H_2.

Table 2: Vibrations of the intermediate observed by in situ IR spectroscopy and computed vibrations for an axeq- and eqeq-coordinated acyl complex.

	Expt. [cm^{-1}][a]	eqeq [cm^{-1}][b]	axeq [cm^{-1}][b]
CO_{eq}	2040	*2031* (2113)	–
$CO_{eq\text{-}eq}$	2004		*1987*(2067)
CO_{ax}	1969	*1968* (2048)	–
CO_{eq+eq}	1956	–	*1949* (2028)
CO_{acyl}	1663	*1667* (1734)	*1704* (1773)

[a] Si-comp, toluene [10^{-2} M]. [b] B3LYP/6-31G(d,p)[C,H,N,O,P] + LANL2DZ[Rh], the values in italics are obtained by anharmonic correction.

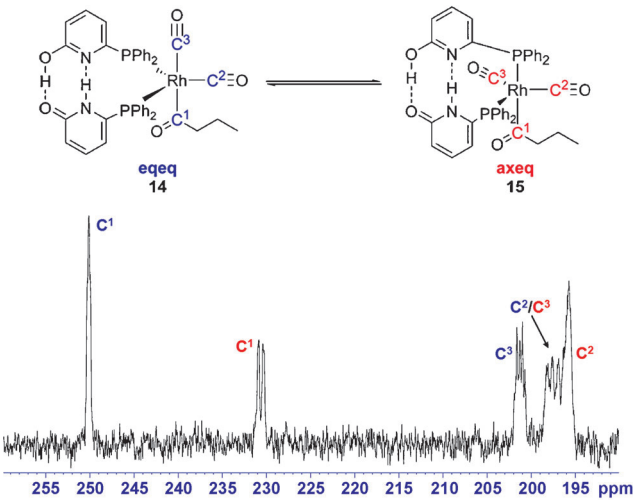

Figure 6. ^{13}C NMR spectrum of the intermediate (193 K, 500 MHz).

Table 3: Comparison of the experimentally observed ^{13}C NMR shifts of the intermediate and the computed shielding.

	Expt. [ppm]	eqeq [ppm][a]	axeq [ppm][a]
$C3_{axeq}$	195.7	–	188.9
$C2_{axeq/eqeq}$	197.6	192.2	192.4
$C3_{eqeq}$	201.3	196.0	–
$C1_{axeq}$	230.6	–	234.9
$C1_{eqeq}$	250.1	248.5	–

[a] M06/6-311+G(2d,p)[C,H,N,O,P]+SDD[Rh] on B3LYP/6-31G(d,p)[C,H,N,O,P]+LANL2DZ[Rh] optimized structures referenced to $[HRh(PPh_3)_3(CO)]$ ($\delta = 206.8$ ppm).[25]

Table 4: Comparison of the experimentally observed ^{1}H NMR spectroscopic shifts of the intermediate and the computed shielding.

	Expt. [ppm]	eqeq [ppm][a]	axeq [ppm][a]
$H2_{axeq}$	13.79	–	13.71
$H1_{eqeq}$	13.45	13.33	–
$H1_{axeq}$	13.05	–	12.91
$H2_{eqeq}$	12.90	12.71	–

[a] M06/6-311+G(2d,p)[C,H,N,O,P]+SDD[Rh] on B3LYP/6-31G(d,p)[C,H,N,O,P]+LANL2DZ[Rh] optimized structures referenced to tetramethylsilane ($\delta = 0.00$ ppm).

stretching vibration (1734 cm^{-1}, Figure 5).[22,23] To investigate the presence of hydrogen bonding in this intermediate by NMR spectroscopy, we performed the experiment described previously with ^{13}C-labeled CO in $[D_8]$toluene. After the same IR spectroscopic signature was observed (taking into account the frequency shift of the CO vibrations because of the isotopic labeling[8]), a sample was removed for low-temperature NMR experiments.[24] The ^{13}C NMR spectrum shows signals at 250.1 ppm and 230.6 ppm, which can be assigned to the acyl carbon atoms of the eqeq-(**14**) and *axeq*-coordinated (**15**) rhodium–acyl complexes (C^1 in Figure 6).

The computed chemical shifts for **14** and **15** are in excellent agreement with the experimental value (Tables 3 and 4). The ^{31}P NMR spectrum recorded at 193 K shows five signals corresponding to a rhodium-bound ligand and one signal for the free ligand **3**, which is present as one equivalent of **3** was replaced by CO when starting from **4**.[8] As expected, the signals assigned to the acyl carbon atoms show HMBC cross-peaks to the neighboring CH_2 signals (Figure 7).

If, as assumed, hydrogen bonding occurs in acyl complexes **14** and **15**, hydrogen-bond signals (10–15 ppm) should be observable in a 1:2 ratio relative to the CH_2 group. Indeed, four signals in the hydrogen-bond region could be detected and assigned by DFT calculations to the N–H···N and O–H···O hydrogen bonds of **14** and **15** (Figure 8). The broad signal at 12.6 ppm corresponds to the N–H···O proton of **3**, which forms symmetrical pyridone dimers. Interestingly, integration of the CH_2 group of the acyl residue suggests that the *axeq* complex is slightly preferred. This preference is in agreement with M06 single-point calculations ($\Delta E = 0.9$ kcal mol^{-1}) on the B3LYP-optimized structures.

In summary, we have demonstrated that the hydrogen-bonding network of the 6-DPPon (**3**) system enhances the activity and selectivity of the hydroformylation of 1-octene. To ensure that hydrogen bonding is not only present in the resting state but throughout the catalytic cycle, a catalytically competent intermediate (proven by in situ IR studies) was characterized. The existence of hydrogen bonds was verified unambiguously through correlation of ^{1}H and ^{13}C NMR spectroscopy supported by DFT calculations. These results show that the outstanding activity and selectivity of the 6-DPPon (**3**) self-assembly catalyst is a direct consequence of

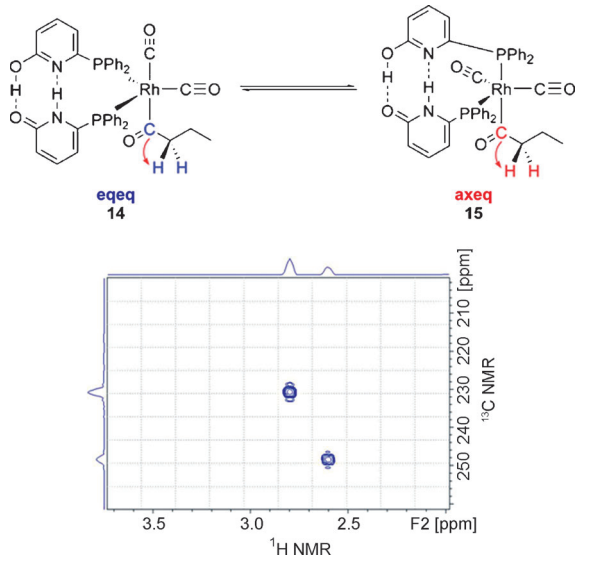

Figure 7. HMBC spectrum (253 K, 500 MHz) which shows the relationship between the acyl carbon atoms of **10** and **11** and the neighboring CH_2 groups.

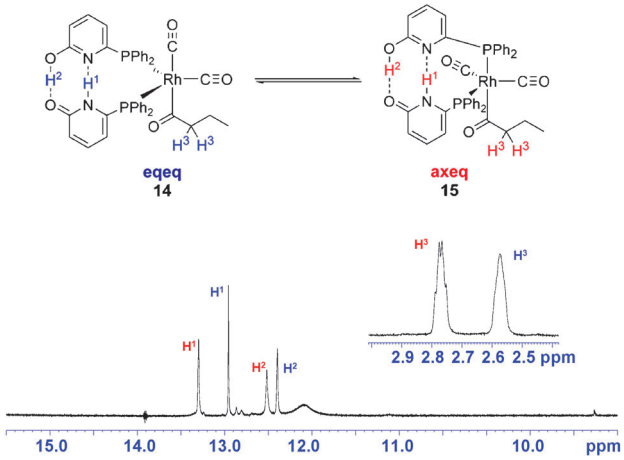

Figure 8. ^{1}H NMR spectrum of the intermediate (253 K, 500 MHz).

the hydrogen-bonding interaction of the ligand. The hydrogen bonding provides a synergism of flexibility and structural integrity which facilitates the adoption of different coordination geometries without a significant energy penalty whilst maintaining the regiodiscriminating properties of a chelating ligand. The findings reported herein should assist in the rational design of future supramolecular catalysts.

Received: May 16, 2012
Published online: September 28, 2012

Keywords: DFT calculations · hydroformylation · hydrogen bonds · IR spectroscopy · self-assembly

[1] a) K. Weissermel, H.-J. Arpe, *Industrial Organic Chemistry*, Wiley-VCH, Weinheim, **2003**, pp. 127–144; b) B. Breit, *Top. Curr. Chem.* **2008**, *279*, 139–172; B. Breit, W. Seiche, *Synthesis* **2001**, 1–36; c) *Rhodium Catalyzed Hydroformylation* (Eds.: P. W. N. M. van Leeuwen, C. Claver), Kluwer Academic, Dordrecht, **2000**.

[2] a) M. Kranenburg, Y. E. M. van der Burgt, P. C. J. Kamer, P. W. N. M. van Leeuwen, *Organometallics* **1995**, *14*, 3081–3089; b) T. J. Devon, G. W. Philips, T. A. Puckette, J. L. Stavinoha, J. J. Vanderbilt, US Patent 4 694 109, **1988**; c) E. Billig, A. G. Abatjoglou, D. R. Bryant, US Patent 4 769 498, **1988**; d) G. D. Cunny, S. L. Buchwald, *J. Am. Chem. Soc.* **1992**, *114*, 5535–5543.

[3] a) W. Seiche, B. Breit, *J. Am. Chem. Soc.* **2003**, *125*, 6608–6609; b) W. Seiche, A. Schuschkowski, B. Breit, *Adv. Synth. Catal.* **2005**, *347*, 1488–1494; c) C. Waloch, J. Wieland, M. Keller, B. Breit, *Angew. Chem.* **2007**, *119*, 3097–3099; *Angew. Chem. Int. Ed.* **2007**, *46*, 3037–3039.

[4] For other approaches to supramolecular catalysis, see a) P. Dydio, W. I. Dzik, B. de Bruin, J. N. H. Reek, *Angew. Chem.* **2011**, *123*, 416–420; *Angew. Chem. Int. Ed.* **2011**, *50*, 396–400; b) M. Kuil, T. Soltner, P. W. N. M. van Leeuwen, J. N. H. Reek, *J. Am. Chem. Soc.* **2006**, *128*, 11344–11345; c) T. S. Koblenz, J. Wassenaar, J. N. H. Reek, *Chem. Soc. Rev.* **2008**, *37*, 247–262; d) L. Diab, T. Smejkal, J. Geier, B. Breit, *Angew. Chem.* **2009**, *121*, 8166–8170; *Angew. Chem. Int. Ed.* **2009**, *48*, 8022–8026; e) A. W. Kleij, M. Lutz, A. L. Spek, P. W. N. M. van Leeuwen, J. N. H. Reek, *Chem. Commun.* **2005**, 3661–3663; f) V. F. Slagt, P. C. J. Kamer, P. W. N. M. van Leeuwen, J. N. H. Reek, *J. Am. Chem. Soc.* **2004**, *126*, 1526–1536; g) V. F. Slagt, J. N. H. Reek, P. C. J. Kamer, P. W. N. M. van Leeuwen, *Angew. Chem.* **2001**, *113*, 4401–4404; *Angew. Chem. Int. Ed.* **2001**, *40*, 4271–4274; h) J. M. Takacs, D. S. Reddy, S. A. Moteki, D. Wu, H. Palencia, *J. Am. Chem. Soc.* **2004**, *126*, 4494–4495; i) P. W. N. M. van Leeuwen, D. Rivillo, M. Raynal, Z. Freixa, *J. Am. Chem. Soc.* **2011**, *133*, 18562–18565.

[5] O. Abillard, B. Breit, *Adv. Synth. Catal.* **2007**, *349*, 1891–1895.

[6] D. Fuchs, G. Rousseau, L. Diab, U. Gellrich, B. Breit, *Angew. Chem.* **2012**, *124*, 2220–2224; *Angew. Chem. Int. Ed.* **2012**, *51*, 2178–2182.

[7] U. Gellrich, J. Huang, W. Seiche, M. Keller, M. Meuwly, B. Breit, *J. Am. Chem. Soc.* **2011**, *133*, 964–975.

[8] The spectra are shown and discussed in detail in the Supporting Information.

[9] Kinetic studies revealed a first order dependency of the alkene concentration, thus suggesting that either alkene coordination or hydrometalation is rate-determining. For details, see the Supporting Information.

[10] All calculations were performed with Gaussian 09: M. J. Frisch et al., Gauusian 09 Rev. B.01, Gaussian, Inc., Wallingford CT, **2010**. The complete reference, alternative pathways, and details of the calculations are reported in the Supporting Information.

[11] See for example: a) J. J. Carbó, F. Maseras, C. Bo, P. W. N. M. van Leeuwen, *J. Am. Chem. Soc.* **2001**, *123*, 7630–7637; b) R. Lazzaroni, R. Settambolo, G. Alagona, C. Ghio, *Coord. Chem. Rev.* **2010**, *254*, 696–706.

[12] Energy barriers for the coordination of ethene to model phosphane-modified systems: D. Gleich, J. Hutter, *Chem. Eur. J.* **2004**, *10*, 2435–2444; an energy barrier for the coordination of ethene to thixantphos-modified rhodium catalysts has been reported, but only a barrier for coordination to the *cis* complex could be located and a barrierless coordination to the *trans* complex was reported: E. Zuidema, L. Escorihuela, T. Eichelsheim, J. J. Carbó, C. Bo, P. C. J. Kamer, P. W. N. M. van Leeuwen, *Chem. Eur. J.* **2008**, *14*, 1843–1853.

[13] Additional confomers of **5** and **6** were optimized in which hydrogen bonding is prevented for geometrical reasons, but these confomers are predicted to be 8.2 kcal mol^{-1} and 4.8 kcal mol^{-1}, respectively, higher in energy by the M06//B3LYP level of theory.

[14] a) J. Uddin, C. R. Landis, *J. Chem. Soc. Dalton Trans.* **2002**, 729 – 742; b) see Ref. [12].
[15] For a detailed analysis of the different possible alkene complexes and the resulting transition states see Figure S27 in the Supporting Information.
[16] J. Wassenaar, E. Jansen, W.-J. van Zeist, F. M. Bickelhaupt, M. A. Siegler, A. L. Spek, J. N. H. Reek, *Nat. Chem.* **2010**, *2*, 417 – 421.
[17] By taking the pre-equilibria between **6** and **7** into account, for example, regarding a $k_{eff} = k_{\mathbf{6}\rightarrow\mathbf{7}}k_{\mathbf{7}\rightarrow\mathbf{8}}/(k_{\mathbf{6}\rightarrow\mathbf{7}}+k_{\mathbf{7}\rightarrow\mathbf{6}})$ relationship for the two pathways, a selectivity of 89:11 is computed at the M06//B3LYP level.
[18] To ensure that the same catalytic active species is present we followed this reaction by in situ IR spectroscopy: a) R. Lazzaroni, G. Uccello-Baretta, M. Benetti, *Organometallics* **1989**, *8*, 2323 – 2327; b) P. C. Casey, L. M. Petrovich, *J. Am. Chem. Soc.* **1995**, *117*, 6007 – 6014; c) S. C. van der Slot, P. C. J. Kamer, P. W. N. M. van Leuween, J. A. Iggo, B. T. Heaton, *Organometallics* **2001**, *20*, 430 – 441.
[19] The results of the hydroformylation in terms of dependency on the CO/H_2 pressure can be found in the Supporting Information.
[20] For the synthesis of these ligands, see reference [7].
[21] J. Feng, M. Garland, *Organometallics* **1999**, *18*, 417 – 427.
[22] P. C. J. Kamer, A. van Rooy, G. C. Schoemaker, P. W. N. M. van Leeuwen, *Coord. Chem. Rev.* **2004**, *248*, 2409 – 2424.
[23] Recently, we (C. H. Beierlein, R. A. Paz-Schmidt, D. A. Plattner, B. Breit, *Organometallics* **2010**, *29*, 2521 – 2532) and others (J. Meeuwissen, A. J. Sandee, B. de Bruin, M. A. Siegler, A. L. Spek, J. N. H. Reek, *Organometallics* **2010**, *29*, 2413 – 2421) discussed the possibility of an insertion of the rhodium atom into a γ- or β-NH bond of the ligand, thereby resulting in a rhodium hydride species that is able to undergo reductive elimination. We were able to locate a TS for rhodium insertion into a N–H bond, but the computed barrier renders this process unlikely to happen (see the Supporting Information). This is in agreement with the in situ IR experiments, which show that by using 1.5 equivalents of 1-octene the formation of nonanal occurs only after pressurizing the solution with H_2 (see Figure 5).
[24] For NMR studies of rhodium–acyl complexes, see a) A. G. Kent, J. M. Brown, *J. Chem. Soc. Perkin Trans. 2* **1988**, 1587 – 1607; b) see Ref. [18c].
[25] J. M. Brown, L. R. Canning, A. G. Kent, P. J. Sidebottom, *J. Chem. Soc. Chem. Commun.* **1982**, 721 – 723.

